Magnetic reconnection configurations and particle acceleration in solar flares

P. F. Chen, W. J. Liu, C. Fang

Department of Astronomy, Nanjing University, Nanjing 210093, China

Abstract

Numerical simulations of two types of flares indicate that magnetic reconnection can provide environments favorable for various particle acceleration mechanisms to work. This paper reviews recent test particle simulations of DC electric field mechanism, and discusses how the flare particles can escape into the interplanetary space under different magnetic configurations.

Key words:
solar flares, magnetic reconnection, particle acceleration
PACS: 96.60.qe, 96.60.Iv, 96.50.Pw

1 Introduction

Energetic particles are of significant interest to the solar community not only because they can provide the unique information about the physics of the solar eruptions, but also are an important driver for hazardous space weather conditions. Three mechanisms have been proposed for the acceleration of energetic particles, i.e., electric DC-field acceleration, wave turbulence (or stochastic) acceleration, and shock acceleration (see Miller et al., 1997; Aschwanden, 2002, for a review). Magnetic reconnection, as the mechanism of solar flares, provides favorite environments for all of them to work.

Solar flares are associated with the release of a huge amount of magnetic energy, which is distributed into kinetic energy, strong radiation of the plasma, as well as energetic nonthermal particles. Magnetic reconnection has been established to play an essential role in these processes. Traditionally, solar flares
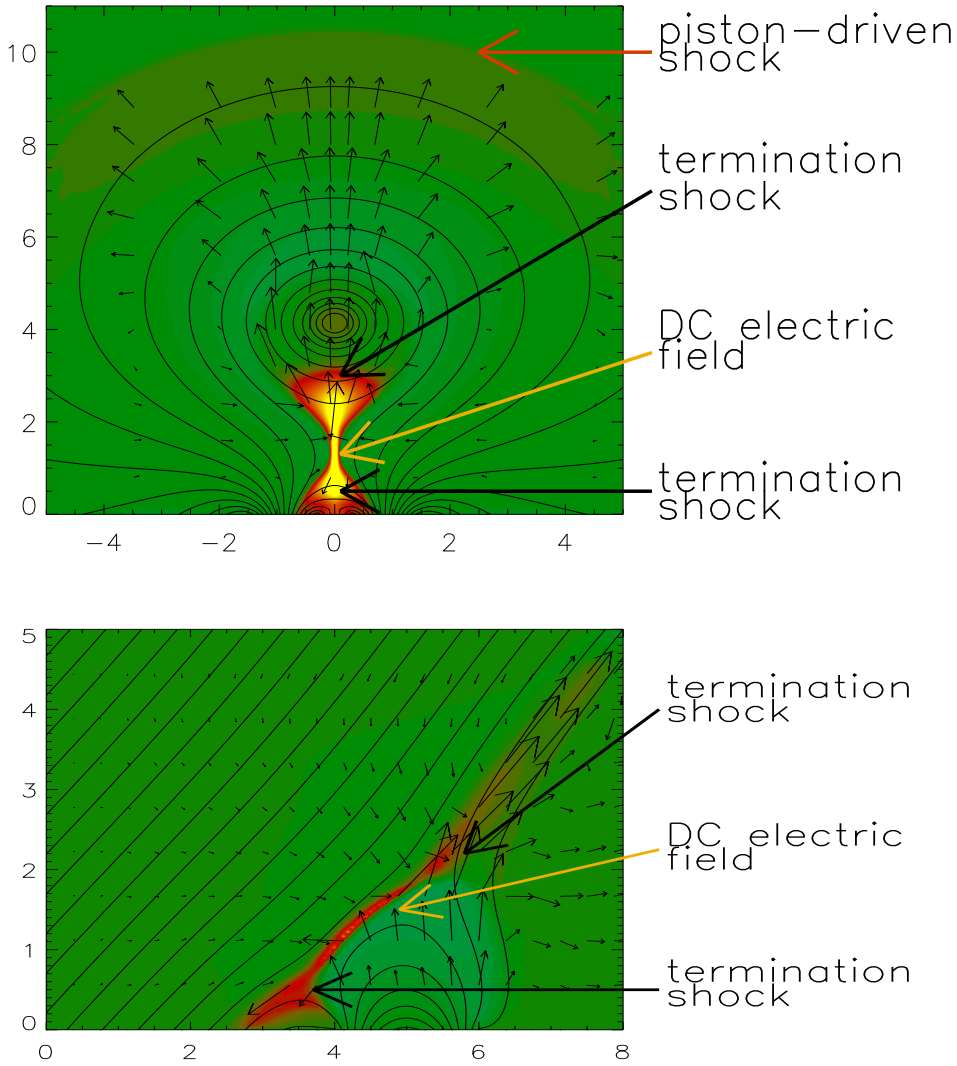
Fig. 1. Numerical simulations of two types of solar flares. Upper panel: two-ribbon flares; Lower panel: compact flares. The color shows the temperature, solid lines correspond to the magnetic field lines, and arrows to the velocity field.

are divided into two types, i.e., two-ribbon and compact flares. Two-ribbon flares are often associated with filament eruptions and/or coronal mass ejections (CMEs). It is believed in the so-called CSHKP model that, a filament, or only a flux rope which may not yet host a filament, loses its equilibrium somehow (see Forbes, 2000; Gopalswamy, 2003, for reviews), and a current sheet is formed as the field lines covering the flux rope are stretched up. The reconnection leads to the fast eruption of the filament as the core of a CME, as well as a two-ribbon flare beneath the reconnection site. Based on the strong correlation between emerging flux and filament eruptions (Feynman and Martin, 1995) and the existence of a soft X-ray precursor in many CME events (Harrison et al., 1985), Chen and Shibata (2000) proposed an emerging flux

trigger mechanism for CMEs. The numerical simulation of the triggering process and the following evolution showed a strong DC electric field located at the reconnection site, plenty of turbulent motions in the super-Alfvénic outflow, and three shocks, i.e., a piston-driven shock above the erupting flux rope and two termination shocks located above the flaring loop and immediately beneath the flux rope respectively, as illustrated in the upper panel of Fig. 1. All of them are proxies for particle acceleration. Compact flares, on the other hand, are produced by the reconnection between an emerging flux and preexisting coronal loop (Heyvaerts et al., 1977), or they can be due to loop-loop interaction in the corona (Hanaoka, 1994). The numerical simulation of such a process (e.g., Yokoyama and Shibata, 1995) showed also that a strong DC electric field exists near the reconnection site, turbulent motions associated with the super-Alfvénic outflow, and two termination shocks with one above the flaring loop and another one at the position where upward flow collides with the ambient coronal magnetic field, as illustrated in the lower panel of Fig. 1.

Therefore, it is seen that for both types of solar flares, magnetic reconnection ensures the availability of all the three mechanisms for particle acceleration. While there is no doubt that the piston-driven shock above the erupting flux rope can accelerate particles into relativistic energy, debates are mainly focused on whether the DC electric field, the turbulent motions, or termination shocks associated with magnetic reconnection are responsible for the nonthermal particles that bombard the chromosphere to form hard X- and γ-ray emissions and that propagate to the interplanetary (IP) space to form impulsive solar energetic particle (SEP) events (Nitta et al., 2006). In this paper, we focus on the simulations about the DC electric field mechanism, since in many flare events, bi-directional nonthermal electron beams are found to originate from a very compact region with a size less than 2000 km, as indicated by simultaneous normal and reverse type III radio bursts (Aschwanden et al., 1995). This means that the acceleration region is in the proximity of the reconnection X-point, which makes the DC mechanism very viable, though it is believed that turbulence should also exist near the reconnection site owing to microscopic instabilities (e.g., Lee, 1982; Somov, 1992).

This paper is organized as follows. Section 2 reviews previous test particle simulations on the DC mechanism, and Section 3 describes our recent results in test particle simulations. In Section 4, the escape problem of the energetic particles is discussed, which is followed by the summary of this paper.

3

2 General Results in the Simulations of DC Mechanism

The DC electric field mechanism has been studied extensively in the context of solar flares. Initially it was considered by Holman (1985) and Tsuneta (1985) in order to relate the accelerated electrons to the properties of the thermal plasma and compute the flux of electrons accelerated out of the thermal plasma, where the adopted electric field was not so strong. Recently, observations indicate that the electric field near the reconnection point can reach 1-10 V cm^{-1}, four orders larger than the Dreicer field (Kopp and Poletto, 1986; Foukal et al., 1987). Realizing this fact, Martens (1988) considered the electron and proton acceleration in a strong super-Dreicer field, where the acceleration length becomes about 100 m for electrons and 1000 m for protons, much smaller than their mean free paths. Bulanov (1980), Litvinenko and Somov (1993), Zhu and Parks (1993), and Kaufmann et al. (1994) investigated the role of the longitudinal component of the reconnecting magnetic field, and found that it increases considerably the efficiency of particle acceleration in the current sheet.

Since the acceleration length is much smaller than the mean free path (Martens, 1988), test particle simulation would be a very nice approximation for describing the accelerating process of the particles. For this kind of research, a magnetic field with a typical X-type configuration, and an electric field in the longitudinal direction are often arbitrarily specified independently (see the references in Hamilton et al., 2003). Then up to hundreds of thousand test particles are randomly distributed near the reconnection site, and their independent trajectories are simulated by numerically solving the relativistic equations of momentum, i.e.,

$$\frac{d(\gamma m_0 \mathbf{v})}{dt} = q\mathbf{E} + q\mathbf{v} \times \mathbf{B}, \tag{1}$$

$$\frac{d\mathbf{x}}{dt} = \mathbf{v}, \tag{2}$$

where γ is the Lorentz factor.

An improvement was made with respect to the specification of the electric field by using the Ohm's law (e.g., Petkaki and MacKinnon, 1997; Hamilton et al., 2003; Zharkova and Gordovskyy, 2004; Wood and Neukirch, 2005), which makes the electric field distribution more or less self-consistent with the reconnecting magnetic field.

The main results are that: (1) a certain amount of particles are accelerated and then propagate along the separatrix lines (Hannah et al., 2002; Dalla and Browning, 2005) (note that the particle acceleration in Dalla and Browning,

2005 is more like the betatron mechanism); (2) it is possible for electrons to be accelerated up to 100 keV and for protons to 100 MeV; (3) The energy spectrum of the accelerated particles shows a typical power-law distribution, i.e., the number density N scales with the energy E as $N \propto E^{-\delta}$. The spectral index, δ, varies from 1.3 to 2 for electrons (Fletcher and Petkaki, 1997; Vekstein and Browning, 1997; Zharkova and Gordovskyy, 2005; Wood and Neukirch, 2005) and from 0.92 to 2 for protons (Mori et al., 1998; Heerikhuisen et al., 2002; Hamilton et al., 2003).

It is pointed out that whether the total number of accelerated particles is comparable with observations remains an open question despite various efforts as discussed in Wood and Neukirch (2005), and more efforts should also be made to address other fundamental issues, such as the heavy ion enhancements (Miller et al., 1997).

3 Effect of Magnetic Parameters on the Energy Spectrum

As seen in Section 2, test particle simulations in various groups obtained quite similar results. For example, the spectral indices for both electrons and protons roughly fall in the range between 0.9 and 2.2. This could explain the hard photon spectrum in the γ-ray range, while it is not compatible with the spectral indices in the hard X-ray range, i.e., between 3 and 7 in a majority of events observed by RHESSI, which requires that the corresponding spectral index of the injected electron flux should be between 4 and 8 assuming a thick-target model (Brown , 1971).

Several factors may be attributed to the big discrepancy. First of all, few simulations were performed with a self-consistent electro-magnetic field which fully satisfies the MHD equations. Second, magnetic configuration parameters were chosen randomly due to our poor knowledge of the actual properties in the reconnecting current sheet in solar flares. Finally, the neglect of the thermalization via Coulomb collisions would lead to a harder energy spectrum. The big difference of the spectral indices between simulations and observations provoked us to investigate the dependence of the spectral index on magnetic configuration parameters using a self-consistent electro-magnetic field which is obtained from numerical simulations of the resistive MHD equations (the details will be presented in Liu et al., 2007): Following Chen et al. (1999), a reconnecting current sheet with the following initial magnetic configuration is numerically simulated with the same 2.5D resistive MHD code:

$$B_x = 0, \tag{3}$$

$$B_y = \begin{cases} |x|/x, & |x| \geq w, \\ \sin[\pi x/(2w)], & |x| < w, \end{cases} \tag{4}$$

$$B_z = \begin{cases} c, & |x| \geq w, \\ \sqrt{c^2 + \cos[\pi x/(2w)]}, & |x| < w, \end{cases} \tag{5}$$

where w is the half-width of the current sheet and c is a constant.

When the reconnection approaches a quasi-steady state, the electro-magnetic field is adopted for the test particle simulations, where 10^5 electrons are uniformly distributed near the reconnection X-point. The magnetic configuration parameters considered here include the strength of the reconnecting magnetic field, which is represented by the plasma β, the width of the current sheet (L_0, note that the thickness of the current sheet is 1.1 times as large as its width in the simulations), and the longitudinal component of the magnetic field (B_z). Fig. 2 shows a typical energy spectrum of electrons when they propagate beyond the resistivity region. It is found that the double power-law (or knee) distribution as in this figure is a common feature (it should be noted that the spectral profile in the range 20-140 keV can also be well fitted to an exponential distribution as in Anastasiadis et al. 2004, see Liu et al. 2007 for detailed discussions). The physical reason of the double power-law could be related to the nonuniform distribution of the electric field in the MHD simulations, i.e., the stronger but narrow electric field near the X-point contributes to the higher energy part, while, the weaker but wide electric field further out to the lower energy part. The two parts are fitted to two power law spectra in order to get the corresponding indices. Since the spectral index at the lower energy remains ~ 1.3, which is almost independent of the above free parameters, we take the spectrum above the break point into consideration, the dependence of the spectral index (δ) on the magnetic configuration parameters is illustrated in Fig. 3. It can be seen that δ decreases as the length scale increases; similar variation holds for the magnetic field, i.e., the stronger the magnetic field, the smaller δ; while the effect of B_z is not monotonic, as shown in the right panel. It is noted that the spectral indices in our simulations are mucher larger than in previous research, which is possibly due to the usage of a self-consistent electro-magnetic field and the shorter thickness of the current sheet. Whether such a self-consistent electro-magnetic field can reproduce the characteristics of protons and heavy ions in solar flares and SEP events is under investigation.

4   Escaping Problem for Accelerated Particles

Our parameter survey in the previous section indicates that with certain parameters the DC mechanism can reproduce the spectral index of the energy spectrum required from observations of the hard X-ray emissions, which are produced when downward particles bombard the solar chromosphere. But, at the same time, roughly similar amount of particles are injected upward, and
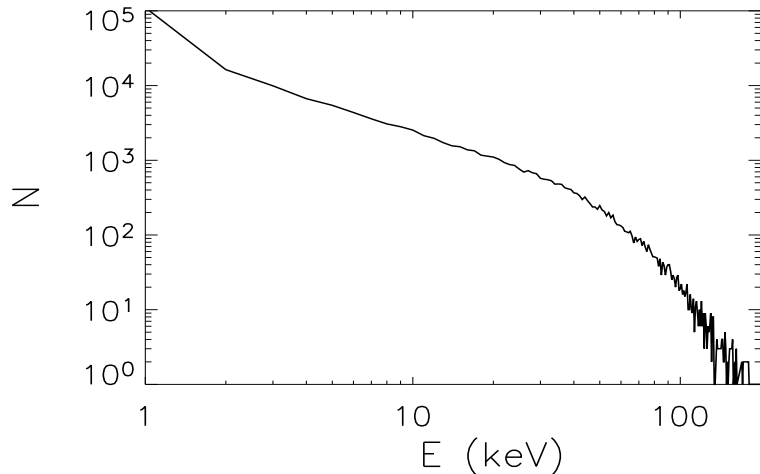
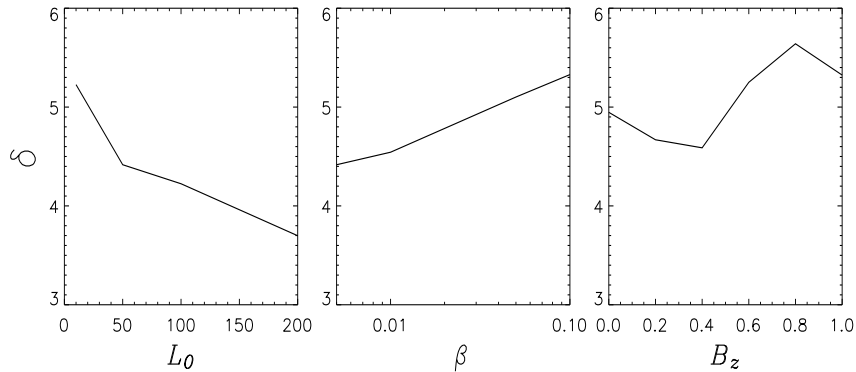Fig. 2. The energy spectrum of electrons in the case when B_z=1 G, β=0.01, and L_0=100 m.

Fig. 3. Variations of the energy spectral index of electrons with the length-scale, L_0 (*left panel*, where $B_z = 1.0$ and $\beta = 0.005$), the plasma β, (*middle panel*, where $L_0 = 50$ m and $B_z = 1.0$), and the z-component of the reconnecting magnetic field, B_z (*right panel*, where $L_0 = 50$ m and $\beta = 0.1$).

these particle may propagate into the IP space to form SEP events.

In accord with the two types of solar flares in the low corona, there are also two types of SEP events in the IP space, i.e, impulsive and gradual SEP events (Reames, 1995). It is generally believed that the impulsive SEP events correspond to the impulsive (or compact) solar flares, while gradual SEP events to two-ribbon flares. In the impulsive flare case, when emerging flux or a moving coronal loop reconnects with another coronal loops, the DC accelerated particles are probably trapped in the loops; while when they reconnect with open field lines, the DC-accelerated particles can then easily escape into the IP space along the open field lines as shown in the lower panel of Fig. 1. The upward reconnection outflow is also guided by the open field lines, which could

7

be observed as a narrow CME by coronagraphs (Kahler et al., 2001). Since the strong electric field lasts for a short time as implied by the short period of hard X-ray emissions, the resulting SEP event has an impulsive time profile. In the two-ribbon flare case, a piston-driven shock straddles over the erupting CME, propagating out rapidly. Particles are accelerated by this fast-mode shock wave and/or the turbulence in the upstream and downstream associated with the shock. These particles are injected into the upstream of the shock and the IP space. Since the shock persists all the way through the IP space with a varying strength, the energetic particles continually accelerated by the shock lead to a gradual SEP event. Therefore, particles, accelerated either by the DC electric field in the impulsive flares or by the piston-driven shock wave in the two-ribbon flares, can both escape into the IP space, leading to impulsive and gradual SEP events, respectively. However, it is often found that there is an impulsive component superposed on the gradual SEP events, which is strongly related to the flaring process. Hence it is believed to be produced by magnetic reconnection (e.g., Cane et al., 2003; Dai et al., 2005). The problem is that in the classical CSHKP model, as shown in the upper panel of Fig. 1, the reconnecting field lines are self-closed. Therefore, it was widely believed that the particles accelerated in the flare are trapped in the closed loops, and while they can bombard the chromosphere, they cannot escape to the IP space (Reames, 2002).

There are several possibilities to overcome the obstacle. One possibility is that the particles may experience pitch-angle scattering and manage their way across the closed field lines to the open field where they can escape, as illustrated by the left panel of Fig. 4. However, considering the collision frequency, such a possibility would be quite small although test particle simulations with pitch-angle scatterings considered are required for further investigations. The second possibility is that actually the classical CSHKP model with all field lines closed is just a local model. The magnetic system could be embedded in a background with open fields, as illustrated by the middle panel of Fig. 4. During the time when the closed field lines are reconnecting, all accelerated particles are trapped in the closed field lines. However, after all the closed field lines have been reconnected, the anti-parallel open field lines begin to reconnect, and the particle accelerated by the DC electric field can then escape along the open field to the IP space. The initiation time of SEP event in this scenario lags behind that of the flare, and the delay can be short or long, depending on total flux of the closed magnetic field lines. This process is somewhat similar to the 3D scenario discussed by Spicer et al. (2006). For the above two possibilities, the DC-accelerated particles may get a chance to be re-accelerated by the piston-driven shock above the erupting flux rope. The third possibility is also related to the open field in the background of the flux rope system. In the emerging flux trigger mechanism proposed by Chen and Shibata (2000) for CMEs as mentioned in Section 1, one of the two scenarios is that the emerging flux appears outside the filament channel and reconnects
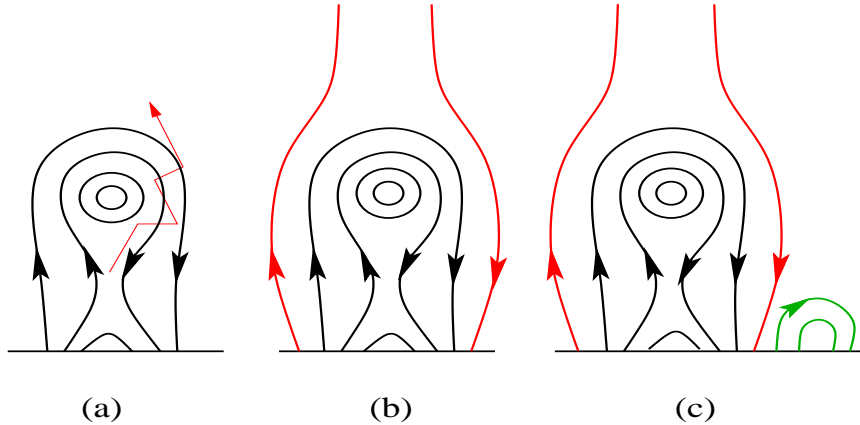
Fig. 4. Three possibilities for the flare particles to escape into the interplanetary space: (a) Particles experience pitch-angle scattering from the reconnection site to the open field; (b) When the open field lines begin to reconnect after all the closed field lines are reconnected, particles escape directly along the open field; (c) As a trigger, an emerging flux reconnects with the open field near a filament channel. The reconnection accelerates particles, which can escape along the open field.

with the ambient coronal field, leading to the loss of equilibrium of the flux rope system. Such a small-scale reconnection process, which leads to the soft X-ray precursor well before the main flare, may also accelerate particles. If the ambient coronal field happens to be open, these particles can propagate into the IP space along the open field lines, as illustrated in the right panel of Fig. 4. This possibility is reenforced by recent observational evidence of the nonthermal emissions associated with a precursor before a flare event (Chifor et al., 2006), which indicates that energetic particles are generated even in the weak reconnection process.

To summarize, in this paper, we illustrated that magnetic reconnection provides the favorite environments for all three particle acceleration mechanisms to work. Since it is still an open question how DC electric field, turbulence, and even termination shocks play their roles in particle acceleration associated with X-ray emissions and the impulsive SEP events, we focused on recent investigations on test particle simulations of DC mechanism, including our very recent parameter survey. These results indicate that DC mechanism can accelerate electrons and protons with the energy spectra constrained by observations. The possibilities for the flare particles to escape into the IP space proposed in this paper deserve further examination in observations.

9

References

Anastasiadis, A., Gontikakis, C., Vilmer, N., Vlahos, L. Electron acceleration and radiation in evolving complex active regions. A&A, 422, 323-330, 2004.

Aschwanden, M. J. Particle acceleration and kinematics in solar flares. Space Sci. Rev., 101, 1-227, 2002.

Aschwanden, M. J., Benz, A. O., Dennis, B. R., Schwartz, R. A. Solar electron beams detected in hard X-rays and radio waves. ApJ, 455, 347-365, 1995.

Brown, J. C. The deduction of energy spectra of non-thermal electrons in flares from the observed dynamic spectra of hard X-ray bursts. Solar Phys., 18, 489-502, 1971.

Bulanov, S. V. The energy spectrum of particles accelerated near a singular magnetic field line Soviet Astron. Lett. 6, 206-208, 1980.

Cane, H. V., von Rosenvinge, T. T., Cohen, C. M. S. et al.Two components in major solar particle events. GRL, 30, SEP 5-1, 2003.

Chen, P. F., Fang, C., Tang, Y. H., Ding, M. D. Flaring loop motion and a unified model for solar flares. ApJ, 513, 516-523, 1999.

Chen, P. F., Shibata, K. An emerging flux trigger mechanism for coronal mass ejections. ApJ, 545, 524-531, 2000.

Chifor, C., Mason, H. E., Tripathi, D., Isobe, H., Asai, A. The early phases of a solar prominence eruption and associated flare: a multi-wavelength analysis. A&A, 458, 965-973, 2006.

Dai, Y., Tang, Y. H., and Qiu, K. P. On some large solar energetic particle events: direct impulsive component and broad associated coronal mass ejections. Adv. Space Res., 35, 1871-1875, 2005.

Dalla, S., Browning, P. K. Particle acceleration at a three-dimensional reconnection site in the solar corona. A&A, 436, 1103-1111, 2005

Feynman, J., Martin, S. F. The initiation of coronal mass ejections by newly emerging magnetic flux. JGR, 100, 3355-3367, 1995.

Fletcher, L., Petkaki, P. Particle acceleration and transport in reconnecting plasmas. Solar Phys. 172, 267-270, 1997.

Forbes, T. G. A review on the genesis of coronal mass ejections. JGR, 105, 23153-23166, 2000.

Foukal, P., Little, R., Gilliam, L. Paschen-line Stark-broadening as an electric field diagnostic in erupting prominences. Solar Phys., 114, 65-73, 1987.

Gopalswamy, N. Coronal mass ejections: Initiation and detection. Adv. Space Res., 31, 869-881, 2003.

Hamilton, B., McClements, K. G., Fletcher, L., Thyagaraja, A. Field-guided proton acceleration at reconnecting x-points in flares. Solar Phys., 214, 339-352, 2003.

Hanaoka, Y. A flare caused by interacting coronal loops. ApJ, 420, L37-L40, 1994.

Hannah, I. G., Fletcher, L., Hendry, M. A. Chaotic dynamics and collisionless reconnection at an X-type neutral point. in Solar Variability: From Core to Outer Frontiers (ESA SP-506; Noordwijk: ESA), 295, 2002.

Harrison, R. A., Waggett, P. W., Bentley, R. D. et al.The X-ray signature of solar coronal mass. Solar Phys., 97, 387-400, 1985.

Heerikhuisen, J., Litvinenko, Yu. E., Craig, I. J. D. Proton acceleration in analytic reconnecting current sheets. ApJ, 566, 512-520, 2002.

Heyvaerts, J., Priest, E, R., Rust, D. M. An emerging flux model for the solar flare phenomenon. 1977, 216, 123-137, 1977.

Holman, G. D. Acceleration of runaway electrons and Joule heating in solar flares. ApJ, 293, 584-594, 1985.

Kaufmann, R. L., Lu, C., Larson, D. J. Cross-tail current, field-aligned current, and By. JGR, 99, 11277-11296, 1994.

Kahler, S. W., Reames, D. V., Sheeley, N. R., Jr. Coronal mass ejections associated with impulsive solar energetic particle events. ApJ, 562, 558-565, 2001

Kopp, R. A., Poletto, G. Magnetic field re-arrangement after prominence eruption. In NASA. Goddard Space Flight Center Coronal and Prominence Plasmas, 469-473, 1986.

Lee, L. C. Ion two-stream and modified two-stream instabilities in the magnetic neutral sheet. Geophys. Res. Lett. 9, 1159-1162, 1982

Litvinenko, Y., Somov, B. Particle acceleration in reconnecting current sheets. Solar Phys. 146, 127-133, 1993.

Liu, W. J., Chen, P. F., Fang, C., Ding, M. D. 2006, ApJ, in preparation.

Martens, P. The generation of proton beams in two-ribbon flares. ApJ, 330, L131-L133, 1988.

Miller, J. A., Cargill, P. J., Emslie, A. et al.Critical issues For understanding particle acceleration in impulsive solar flares. JGR, 102, 14631-14659, 1997.

Mori, K., Sakai, J., Zhao, J. Proton acceleration near an X-type magnetic reconnection region. ApJ, 494, 430-437, 1998.

Nitta, N. V., Reames, D. V., DeRosa, M. L. et al.Solar sources of impulsive solar energetic particle events and their magnetic field connection to the Earth. ApJ, 650, 438-450, 2006.

Petkaki, P., MacKinnon, A. L. Particle acceleration in dynamical collisionless reconnection. Solar Phys. 172, 279-286, 1997.

Reames, D. V. Solar energetic particles: A paradigm shift. Rev. Geophys., 33, 585-590, 1995.

Reames, D. V. Magnetic topology of impulsive and gradual solar energetic particle events. ApJ, 571, L63-L66, 2002.

Somov, B. V. Physical Processes in Solar Flares, Kluwer Academic Publishers, Dordrecht, Holland, Ch. 3, 1992.

Spicer, D. S., Sibeck, D., Thompson, B. J., Davila, J. M. A Kopp-Pneuman-like picture of coronal mass ejections. ApJ, 643, 1304-1316, 2006.

Tsuneta, S. Heating and acceleration processes in hot thermal and impulsive solar flares. ApJ, 290, 353-358, 1985.

Vekstein, G. E., Browning, P. K. Field-aligned particle acceleration in collisionless magnetic reconnection. Phys. Plasmas, 4, 2261-2268, 1997.

Wood, P., Neukirch, T. Electron acceleration in reconnecting current sheets.

Solar Phys., 226, 73-95, 2005.

Yokoyama, T., Shibata, K. Magnetic reconnection as the origin of X-ray jets and halpha surges on the Sun. Nature, 375, 42-44, 1995.

Zharkova, V. V., Gordovskyy, M. Particle acceleration asymmetry in a reconnecting nonneutral current sheet. ApJ, 604, 884-891, 2004.

Zharkova, V. V., Gordovskyy, M. Energy spectra of particles accelerated in a reconnecting current sheet with the guiding magnetic field. MNRAS, 356, 1107-1116, 2005.

Zhu, Z., Parks, G. Particle orbits in model current sheet with a nonzero B(y) component. JGR, 98, 7603-7608, 1993.